JGR Biogeosciences

RESEARCH ARTICLE
10.1029/2019JG005207

Sea Level Rise Explains Changing Carbon Accumulation Rates in a Salt Marsh Over the Past Two Millennia

Nathan McTigue[1], Jenny Davis[1], Antonio B. Rodriguez[2], Brent McKee[2], Anna Atencio[2], and Carolyn Currin[1]

[1]National Centers for Coastal Ocean Science, National Oceanic and Atmospheric Administration, Beaufort, NC, USA, [2]Department of Marine Sciences, University of North Carolina at Chapel Hill, Chapel Hill, NC, USA

Key Points:
- Salt marsh sediment carbon accumulation rate (CAR) varied with local relative sea level rise (RSLR) over the past two millennia
- Over the previous 2,400 years, the highest CAR was during the most recent 150 years, which coincides with the highest RSLR
- The time period to report CAR should be carefully chosen to include contemporary sea level rise but omit labile carbon that will decompose

Correspondence to:
N. McTigue,
mctigue@utexas.edu

Citation:
McTigue, N., Davis, J., Rodriguez, A. B., McKee, B., Atencio, A., & Currin, C. (2019). Sea level rise explains changing carbon accumulation rates in a salt marsh over the past two millennia. *Journal of Geophysical Research: Biogeosciences*, *124*. https://doi.org/10.1029/2019JG005207

Received 12 APR 2019
Accepted 10 AUG 2019
Accepted article online 22 AUG 2019

Author Contributions:
Conceptualization: Nathan McTigue, Jenny Davis, Antonio B. Rodriguez, Brent McKee, Carolyn Currin
Formal analysis: Nathan McTigue
Investigation: Nathan McTigue
Methodology: Antonio B. Rodriguez, Brent McKee, Anna Atencio, Carolyn Currin
Supervision: Carolyn Currin
Visualization: Nathan McTigue
Writing - original draft: Nathan McTigue
Writing – review & editing: Jenny Davis, Antonio B. Rodriguez, Brent McKee, Carolyn Currin

Abstract High rates of carbon burial observed in wetland sediments have garnered attention as a potential "natural fix" to reduce the concentration of carbon dioxide (CO_2) in Earth's atmosphere. A carbon accumulation rate (CAR) can be determined through various methods that integrate a carbon stock over different time periods, ranging from decades to millennia. Our goal was to assess how CAR changed over the lifespan of a salt marsh. We applied a geochronology to a series of salt marsh cores using both ^{14}C and ^{210}Pb markers to calculate CARs that were integrated between 35 and 2,460 years before present. CAR was 39 g $C \cdot m^{-2} \cdot year^{-1}$ when integrated over millennia but was upward of 148 g $C \cdot m^{-2} \cdot year^{-1}$ for the past century. We present additional evidence to account for this variability by linking it to changes in relative sea level rise (RSLR), where higher rates of RSLR were associated with higher CARs. Thus, the CAR calculated for a wetland should integrate timescales that capture the influence of contemporary RSLR. Therefore, caution should be exercised not to utilize a CAR calculated over inappropriately short or long timescales as a current assessment or forecasting tool for the climate change mitigation potential of a wetland.

Plain Language Summary Earth's vegetated habitats convert atmospheric carbon dioxide (CO_2) into plant material, or organic matter (OM), through photosynthesis. In most habitats, OM decomposes back into CO_2 within decades; however, OM that becomes buried in coastal wetland habitats such as salt marshes can resist decomposition for thousands of years. Due to concerns over increasing CO_2 concentrations in the atmosphere, this mechanism, described as the carbon accumulation rate (CAR), has been assessed as a means to naturally remove CO_2 from the atmosphere in hopes of offsetting fossil fuel emissions. Previously calculated rates of OM burial and CAR have been quite variable, making it difficult to calculate the current total burial capacity of the global salt marsh ecosystems. To better understand this process, we measured CAR in a salt marsh and investigated how this rate changed from 2,400 years ago through present time. We found that while the rate of carbon burial was variable, over the lifetime of this marsh it has been closely correlated with local sea level rise. Moving forward, calculation of CAR must accommodate both the influence of sea level rise while also omitting the recently deposited plant material that will decompose and not contribute to long-term OM storage.

1. Introduction

Coastal saline wetlands are recognized for their high productivity, ability to accrete vertically, and capacity to preserve organic carbon (OC) in their sediments for long periods of time (Chmura et al., 2003; Duarte et al., 2005). This unique carbon sequestration and storage capability of vegetated coastal ecosystems, as compared to their terrestrial and freshwater counterparts, has resulted in their designation as "blue carbon" ecosystems (Howard et al., 2017; Mcleod et al., 2011; Nellemann, 2009). Mangrove forests, for example, are among the most carbon-rich tropical forests (~1,000 Mg C/ha) owing to both their aboveground standing biomass and high C content belowground that can be preserved for millennia (Donato et al., 2011). Salt marshes possess stores of carbon up to meters deep that have formed over hundreds to thousands of years (Brevik & Homburg, 2004; Johnson et al., 2007; Redfield, 1965). Redfield's (1965) seminal work recreating the "ontogeny" of a salt marsh by aging multiple depth horizons in a New England salt marsh provided the blueprints for the modern approach to understand coastal geomorphology. Here, we combine that approach with measuring OC stocks to assess the carbon storage capacity of a salt marsh over various time periods.

Coastal wetlands can continually drawdown CO_2 from the atmosphere because of their ability to accrete vertically in response to rising sea level, thus, creating a new volume of sediment in which to accommodate additional organic matter (OM; Rogers et al., 2019). Several ecogeomorphic feedbacks in salt marshes allow them to keep pace with sea level rise (Kirwan & Guntenspergen, 2012). In general, accelerated relative sea level rise (RSLR) causes increased inundation, which leads to enhanced inorganic sediment loading, assuming adequate sediment supply in tidal creeks compared to the position of the marsh platform in the tidal frame (Kirwan & Guntenspergen, 2012; Kirwan & Megonigal, 2013; Pethick, 1981). Sedimentation and accelerated RSLR then promote increased belowground biomass production by the marsh plants (Drexler, 2011; Morris et al., 2002). Together these factors cause vertical marsh accretion and subsequent increased carbon accumulation in sediments (Kirwan & Mudd, 2012). The relationship between accelerating RSLR and increased carbon accumulation in sediments has been affirmed in a recent global synthesis by Rogers et al. (2019). The authors demonstrated that tidal ecosystems that have experienced accelerated RSLR exhibited sediment carbon concentrations 1.7 to 3.7 times higher in their most surficial 20 cm compared to those that have experienced stable sea level in the same timeframe. Notably though, even low rates of RSLR can cause marshes below their optimum growth elevations to drown (Kirwan & Megonigal, 2013). However, where no barriers to the upland exist and the landward gradient is shallow, a salt marsh can transgress landward as higher inundation elevations create new intertidal habitat and vertical accretion will occur provided an adequate supply of sediment (Oertel et al., 1989).

We focus on the rate at which salt marsh OC is shunted into stable belowground pools, referred to here as the carbon accumulation rate (CAR). Various methods exist to measure CAR (Choi & Wang, 2004). One approach measures vertical accretion as a proxy to burial of OM (e.g., feldspar marker horizons and sediment elevation tables), while others integrate a C inventory over the age of a sediment horizon that has been dated using radioisotopes (e.g., ^{137}Cs, ^{210}Pb, and ^{14}C). All methods that measure CAR standardize their rate per annum, yet the actual time periods the rate integrates can vary from years to millennia (e.g., years to decades for feldspar marker horizons, since 1963 for ^{137}Cs, up to ~150 years for ^{210}Pb, and >10,000 years for ^{14}C).

Salt marsh CAR exhibits a wide range of values. Ouyang and Lee (2014), who expanded the meta-analysis of Chmura et al. (2003), report an average salt marsh CAR of 244 g C·m^{-2}·year^{-1} from methods that include ^{137}Cs, ^{210}Pb, and ^{14}C dating and feldspar marker horizons. However, the CARs they surveyed ranged from 3–1,713 g C·m^{-2}·year^{-1} and possessed a right-tailed distribution with a median rate of 139 g C·m^{-2}·year^{-1}. A shorter time used to derive CAR might bias the rate by including labile OC that will later decompose and return to CO_2 within annual to decadal timescales (Davis et al., 2015). For example, some of the highest CARs reported by Ouyang and Lee (2014) were measured using ^{137}Cs or feldspar marker horizons, two approaches that employ relatively short timescales (<50 years) for CAR derivation. This range of salt marsh CAR, spanning three orders of magnitude, has led to uncertainty in assessing the long-term carbon sink potential of blue carbon ecosystems, which have recently garnered attention for their potential role in climate change mitigation as a CO_2 sink (Crooks et al., 2011; Mcleod et al., 2011; Trumper et al., 2009). Moreover, it has been specified as a knowledge gap that requires further investigation (Howard et al., 2017).

Aside from methodological nuances, physical (e.g., compaction and erosion) and biological (e.g., decomposition and root production) factors can affect CAR. Utilizing long cores and/or dating multiple horizons will better incorporate these events into the CAR calculation, whereas shorter cores will represent a more recent snapshot of CAR that may have been modulated by physical and/or biological drivers. It is well known that net sediment accumulation rates decrease with increasing time span across subtidal and terrestrial depositional environments mainly due to discontinuous sedimentation (Sadler, 1981). Sediment accumulation of salt marsh strata, however, has been shown by many researchers to be continuous over decadal to millennial timescales (e.g., Gehrels, 1999; Kemp et al., 2017; van de Plassche et al., 1998) mainly due to salt marshes having a high resistance to erosion (Neumeier & Ciavola, 2004) and a strong positive relationship between accretion and inundation time (Morris et al., 2002; Pethick, 1981).

Stable carbon isotope ratios (δ^{13}C) are a useful tool to determine the provenance of OM deposited in salt marshes (Cloern et al., 2002; Lamb et al., 2006). Primary producers that fix different inorganic carbon pools (e.g., freshwater vs. marine) or use different photosynthetic pathways (e.g., C_3 vs. C_4 pathways) can be differentiated by predictably disparate δ^{13}C values. For example, C_3 vegetation like *Juncus roemerianus* exhibits

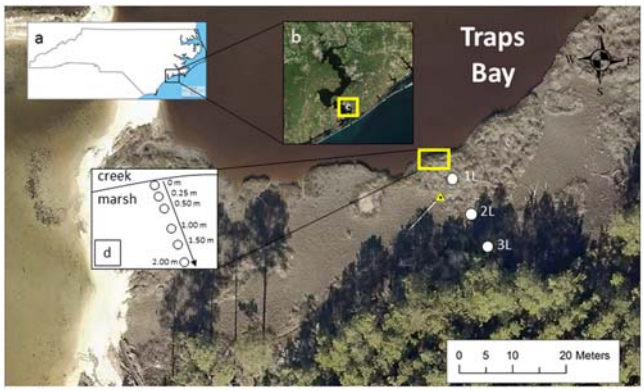

Figure 1. Location of study site within (a) North Carolina, USA, and (b) the New River. Long core locations (white circles) are shown across (c) Traps Bay creek on Marine Corps Base Camp Lejeune. The yellow triangle denotes the location of the Class B elevation benchmark. (d) Short cores were taken within 2 m of the creek bank in line with the long core transect.

relatively ^{13}C-depleted values from −30‰ to −22‰, whereas C_4 vegetation like *Spartina alterniflora* possesses relatively ^{13}C-enriched values from −18‰ to −13‰ (Lamb et al., 2006).

Factors such as salinity, regional climate, water chemistry, soil type, and vegetation can make comparisons of salt marsh carbon stocks complex (Holmquist et al., 2018). Our objective was to investigate how CAR from the same salt marsh might change over time with changing RSLR. In this study, we measure CAR using both ^{14}C and ^{210}Pb that provide timeframes between 35 and over 2,400 years to integrate different carbon stocks over multiple time horizons. We hypothesize that CAR will be highest when measured over the shortest, most recent time frames but will decrease as the time CAR is integrated over lengthens (i.e., a negative relationship). Therefore, the magnitude of the carbon sink depends on the time period investigated. Understanding how CAR has changed over the past millennia in a salt marsh is important to developing strategies to utilize blue carbon habitats to mitigate climate change and to improve models of potential future CAR.

2. Methods

2.1. Sample Collection and Plant Community Surveys

Traps Bay Creek is situated along the southern shore of the New River Estuary, NC, on Marine Corps Base Camp Lejeune (Figure 1). The creek's watershed is ~8 km^2 and drains the sandy paleoshoreline of the last interglacial sea level highstand (Winker & Howard, 1977). The fringing marsh ranges from 20 to 40 m wide from creek bank to upland maritime forest, is mixed *S. alterniflora* and *J. roemerianus*, and experiences ~30-cm mixed semidiurnal tides.

Between 2009 and 2016, emergent plant community structure was assessed in mid-July to early August each year during peak biomass. Percent cover of either *J. roemerianus* or *S. alterniflora* was measured in the same experimental plots each year and recorded as Carolina Vegetation Survey category (Peet et al., 2018). Replicate plots ($n = 5$) were arranged along parallel transects at distances of 0, 10, and 20 m from the creek bank. Mean (and standard deviation) percent cover was determined for all replicates using the numerical maximum percent coverage for each category.

Multiple cores were collected at Traps Bay marsh with various coring devices for subsequent analyses as a component of the Defense Coastal/Estuarine Research Program project (https://dcerp.rti.org/). Three long (L) cores were collected with a stainless steel Russian peat corer (diameter = 5 cm) to the depth of resistance (i.e., the basal paleoshoreline sand unit or marsh contact) since the corer cannot penetrate the basal paleoshoreline sand unit. Depth of the marsh contact varied by core between 90 and 224 cm from the surface (Table 1). We assume no carbon from the current marsh lies below the marsh contact. Cores were arranged along a shoreline-perpendicular transect at distances of 5.6, 12.1, and 16.6 m from the creek bank and are referred to as 1L, 2L, and 3L, respectively (Figure 1). Cores were cut into 1-m long sections and transferred to PVC cradles in the field. Distance from the creek bank was measured by meter tape to the nearest 0.1 m. All core material was similar in consistency in that they contained high proportions of peat with a black-brown sandy mud. Near the surface of the cores, OM was identifiable as fine roots or leafy material, but deeper than 50 cm the core material was mostly fine, unidentifiable organic material mixed with black, sandy mud. In Core 2L from 154 to 160 cm, a woody material was identified. All cores were underlain with a gray-brown fine clayey sand, which we denote as the marsh contact.

One core adjacent to Core 2L, designated Core 2L-Pb, was collected with an aluminum core (7-cm diameter) driven by hand to 50 cm deep for ^{210}Pb geochronology determination. This core was kept intact in the aluminum core tube until sectioning the next day. Additionally, six shorter cores (10–35 cm) were collected with a polycarbonate tube (7-cm diameter) driven into the marsh by hand (Figure 1d). These cores were collected in close proximity to one another (25–50 cm) to create a cross-sectional carbon profile within 2 m of the creek bank.

Table 1
Depths, Ages, Carbon Inventories, and CARs for Long Cores Collected at Traps Bay

Parameter	Core 1L	Core 2L	Core 3L
Surface elevation (NAVD88, m)	0.068	0.082	0.085
Distance from creek bank (m)	5.6	12.1	16.6
Depth of marsh contact (cm)	224	194	90
Depth of ^{14}C sample (cm)	220	—	—
^{14}C age of sample (cal BP)	2330 ± 20	—	—
^{14}C calibrated age of sample (cal BP_{2016})	2416 ± 20[a]	—	—
Age of marsh contact (cal BP_{2016})	2460 ± 20[b]	1970 ± 70[c]	680 ± 80[c]
Carbon stock, entire core (g C·m^{2})	95,575	75,417	33,356
Carbon stock, 0–32 cm (g C·m^{2})	15,279	10,796	11,063
Carbon stock, 0–90 cm (g C·m^{2})	43,507	32,679	—
Carbon stock, 0–194 cm (g C·m^{2})	74,750	—	—
CAR, entire core (g C·m^{-2}·year^{-1})	39 ± 0.3	38 ± 2	49 ± 5
CAR, 0–32 cm (g C·m^{-2}·year^{-1})	141 ± 1.3	100 ± 0.9	102 ± 0.9
CAR, 0–90 cm (g C·m^{-2}·year^{-1})	64 ± 7	48 ± 5	—
CAR, 0–194 cm (g C·m^{-2}·year^{-1})	41 ± 2	—	—

Note. CAR values are arithmetic results ± propagated error from age measurement. A dash indicates no calculation was possible. The age of marsh contact was determined by linear depth-age inference from the depth and age of the actual ^{14}C sample. CAR = carbon accumulation rate.
[a]Calibrated in Calib 7.1 where 0 cal BP is the year CE 1950. Sixty-six years were added so the year CE 2016 is 0 cal BP_{2016}. [b]A linear age-depth extrapolation was used to extend the date of the sample to the depth of the marsh contact. [c]Age was inferred by matching depth of marsh contact to geochronology produced in Kemp et al. (2017). See section 2.4.

At each core location, elevation was measured with a laser level and stadia rod, relative to a Class B benchmark (Figure 1c). The benchmark was a stainless steel rod driven into the ground to the point of refusal, whose elevation (NAVD88) was established via triplicate static GPS collections using the National Geodetic Survey Online Positioning User Service Program.

2.2. Sample Preparation and Analysis for OC Content, ^{13}C, and ^{14}C

Cores collected with the Russian peat corer and with the short polycarbonate tubes were extruded, cut into 2-cm depth intervals, and dried at 60 °C until a constant weight was reached. Once dried and reweighed for bulk density determination, samples were homogenized by hand (mortar and pestle) or mechanically by ball mill (Retsch MM301). A subsample from every 2-cm interval was weighed and ashed at 450 °C for 6 hr to determine OM content (%OM) by loss-on-ignition (Nixon & Oviatt, 1973). A randomized subset of samples underwent elemental analysis (Costech ECS 4010) to determine OC content (%OC) at the National Oceanic and Atmospheric Administration (NOAA) Lab (Beaufort, NC). For analysis of %OC, a homogenized subsample of sediment was subjected to an acidification treatment with 1 M HCl to remove carbonates that would bias the OC content measurement. Using internal acetanilide standards, elemental analysis coefficient of variance was less than 1.5%. Additional subsamples from every 5–10 cm were wrapped in silver capsules, subjected to the acidification procedure described above, dried, and wrapped in an additional tin capsule for bulk stable carbon isotope ratio (δ^{13}C) analysis. This analysis was conducted via continuous flow isotope ratio mass spectrometer on a Thermo Delta V Advantage isotope ratio mass spectrometer coupled to a Costech 4010 elemental analyzer at the University of Connecticut. Raw isotope values were corrected by two-point normalization using U.S. Geological Survey 40 and 41, glutamic acid reference materials. Analytical precision was 0.2‰ or better for δ^{13}C. Stable carbon isotope ratios are reported in standard δ notation relative to the Pee Dee Belemnite standard, where $\delta^{13}C = [(R_{sample}/R_{standard}) - 1] * 1{,}000$, and R is $^{13}C/^{12}C$.

A set of samples ($n = 25$) were analyzed for %OC at both the NOAA Lab and the University of Connecticut for interlaboratory calibration. These samples were highly correlated ($p < 0.001$, $r^2 = 0.97$) and justified our use of data from either lab as one combined data set. Since only some samples were measured for %OC but all were measured for %OM, we derived a site-specific empirical relationship to predict %OC from %OM, based on the approach of Craft et al. (1991). The relationship between %OC and %OM was best fit by a linear

regression ($y = 0.47x + 1.1$, $r^2 = 0.92$), which was subsequently used to convert %OM to %OC and to calculate carbon inventories.

Prior to drying core sections, a macroparticulate OM sample that was clearly identifiable as a single piece of vegetative material was removed from core sections 4, 14, and 24 cm above the basal marsh contact in Cores 1L, 2L, and 3L, respectively (Table 1). The samples were cleaned of extraneous sediment with deionized H_2O under a dissecting scope. Samples were dried at 60 °C in ashed glassware and shipped to the National Ocean Sciences Accelerator Mass Spectrometry lab in Woods Hole, MA, for radiocarbon (^{14}C) age analysis. There samples underwent standard acid-base-acid pretreatment. Samples were converted to graphite and sputtered with heated, ionized Cs to produce ^{12}C, ^{13}C, and ^{14}C ions that were collected in the accelerated mass spectrometry system. The ^{14}C to ^{12}C ratio of the sample was compared to the primary standard of National Bureau of Standards Oxalic Acid I (NIST-SRM-4990). A modern age is defined as 95% of the ^{14}C activity from CE 1950. Various surfaces in the NOAA laboratory were checked for ^{14}C contamination with seven "swab" tests analyzed at the Tritium Lab at the University of Miami and two "swipe" tests analyzed at National Ocean Sciences Accelerator Mass Spectrometry. No contamination was detected.

Radiocarbon ages were calibrated using CALIB 7.1 (Reimer et al., 2013; Stuiver & Polach, 1977) and are reported as the mean probability age rounded to the nearest decade $\pm 2\sigma$. By convention, radiocarbon ages use the year CE 1950 as the modern baseline (Stuiver & Polach, 1977). Thus, to determine the sample's actual age, we added the difference between sample collection date and 1950 (i.e., 66 years for our samples collected in 2016) to the calibrated age and hereafter report ages as calendar years before CE 2016 (cal BP_{2016}).

Sediment carbon density (SCD) was calculated by multiplying the dry bulk density (g/cm^3) of sediment by the OC content (%OC). The SCD ($g\ C/cm^3$) was then multiplied by the depth interval of the sediment section it was measured from to integrate the density to the depth it represents. The mass of carbon per unit area determined for each depth interval was summed and multiplied by 10^4 to produce a depth-integrated carbon stock ($g\ C/m^2$). Sediment CAR ($g\ C \cdot m^{-2} \cdot year^{-1}$) was calculated by dividing carbon stock ($g\ C/m^2$) by the age at the target depth (y). Statistics ($\alpha = 0.05$) and calculations were computed in R 3.4.2 (https://www.r-project.org/). Surface interpolations were created using inverse distance weighting in ArcMap 10.4.1 (Esri Inc., Redlands, CA) and used for qualitative assessment of the carbon cross section of the creek bank.

2.3. ^{210}Pb Geochronology and Analysis via Alpha Spectrometry

The 7-cm diameter core (2L-Pb) was sectioned at 1-cm depth intervals to 50 cm for ^{210}Pb dating via alpha spectrometry. ^{210}Pb is a naturally occurring radioisotope in the ^{238}U decay series with a half-life of 22.3 years. With this short half-life, geochronology using ^{210}Pb allows for high-resolution sediment dating up to 150 years. The total ^{210}Pb activity measured in a sediment sample is partitioned into supported and excess ^{210}Pb. Supported ^{210}Pb ($^{210}Pb_{sup}$) is the ^{210}Pb that is produced in situ by the decay of its parent isotope ^{226}Ra within the particle matrix. $^{210}Pb_{sup}$ is in equilibrium with ^{226}Ra and is generally consistent throughout the sediments of a given area. Excess ^{210}Pb ($^{210}Pb_{xs}$) is the portion of ^{210}Pb that is sorbed onto the particle from surrounding waters and atmosphere. As sediments accumulate, buried sediments do not receive any additional ^{210}Pb, and the buried excess ^{210}Pb decays with time, eventually reaching $^{210}Pb_{sup}$ levels. $^{210}Pb_{sup}$ is calculated by determining the ^{210}Pb deep in the core where concentrations are constant with increasing depth. The mean value within this constant ^{210}Pb activity region is designated as the $^{210}Pb_{sup}$ level. $^{210}Pb_{xs}$ in the depths above is calculated by subtracting $^{210}Pb_{sup}$ from the total ^{210}Pb concentration.

The ^{210}Pb content of the sediments was determined through isotope-dilution alpha spectrometry of the granddaughter isotope, ^{210}Po, which is in secular equilibrium with total ^{210}Pb (El-Daoushy et al., 1991; Flynn, 1968; Matthews et al., 2007). ^{210}Po is a naturally occurring α-emitter with a half-life equal to 128.4 days. The fine fraction of each sample was spiked with ^{209}Po tracer to determine chemical yield. The ^{209}Po activity was determined using the certified natural reference standard IAEA-300. The vessels were microwave digested (Sanchez-Cabeza et al., 1998) at temperatures up to 90 °C. The supernate was separated from the sediments by centrifugation; the sediments were discarded and the supernate was heated to remove nitric acid. Hydrogen peroxide was added to the heated supernate to release organic components (Martin & Hancock, 2004). Once the samples were near dry, ammonium hydroxide was added to precipitate iron. The iron precipitate was separated from the supernate by centrifugation, the supernate discarded, and the precipitate was dissolved with hydrochloric acid to prepare for plating onto stainless steel planchets.

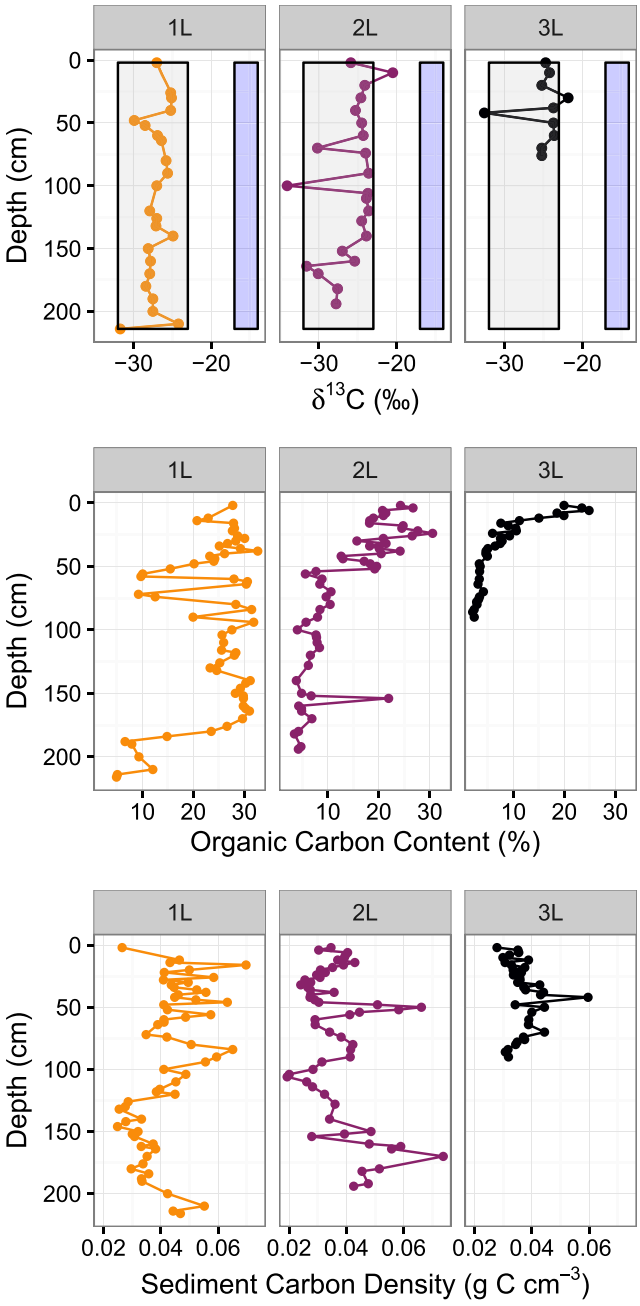

Figure 2. Traps Bay core profiles of stable carbon isotope ratio (top row), organic carbon content (middle row), and sediment carbon density (bottom row). In the top panels, the gray rectangle represents the $\delta^{13}C$ range of C_3 vegetation, while the blue rectangle represents C_4 vegetation (Cloern et al., 2002; Kemp et al., 2010; Lamb et al., 2006).

Ascorbic acid was added to the solution to prevent the iron from interfering with the plating process (Blanchard, 1966; El-Daoushy et al., 1991). After plating, the planchets were analyzed via α-particle spectrometry for 24 hr. The minimum detection limit for alpha-particle spectrometry is ~0.0002 dpm/g, and the analytical uncertainty ranged from 0.5 to 2.0%. Since Core 2L-Pb was collected directly adjacent to Core 2L, the geochronology measured from Core 2L-Pb was applied to the OC stratigraphy measured in Core 2L.

2.4. RSLR and Age Models

Rates of RSLR were calculated from relative sea level data and the age model produced by Kemp et al. (2017) from Cedar Island, NC, which is approximately 90 km northeast of our study site. To investigate if the Cedar Island chronology was applicable to our study site, we compared the age estimates of sediment horizons between Kemp et al. (2017) and those we found using ^{14}C and ^{210}Pb. The marsh sediment depths from Kemp et al. (2017) were reported in Mean Tidal Level (m) but were converted to NAVD88 (m) for comparison to our sites after applying the conversion offset reported from the tide gauge at Beaufort, NC (Station ID: 8656483), which is situated about halfway between the two sites. RSLR rates were calculated from Kemp et al. (2017) as the vertical change in reported historic sea level divided by the difference of median ages. RSLR was plotted against time with locally estimated scatterplot smoothing (LOESS) and 95% confidence interval in R 3.4.2.

3. Results

3.1. Sediment Core Profiles: $\delta^{13}C$, %OC, and SCD

The three cores collected with the peat corer (1L, 2L, and 3L) from Traps Bay were 224, 194, and 90 cm long, respectively (Table 1). The marsh surface elevations of the three cores were within 2 cm relative to each other ranging from 0.068 to 0.085 NAVD88 (m). Sediment OC $\delta^{13}C$ values from all three cores fell between −34.1‰ and −20.5‰, but only two of 55 samples were heavier than −23‰ (Figure 2). OC content ranged from 2.0 to 32.6% for all peat cores at all depths (Figure 2). Much of core 1L contained between 20% and 30% OC. Cores 2L and 3L exhibited higher carbon content in the upper parts of the core, whereas the carbon content was attenuated downcore and approached the lower threshold of measured values.

The SCD of all cores ranged between 0.019 and 0.074 g C/cm^3 (Figure 2). The mean (±s.d.) values for Cores 1L, 2L, and 3L were 0.043 ± 0.010, 0.037 ± 0.011, and 0.037 ± 0.005 g C/cm^3, respectively. SCD showed no pattern with depth in any of the cores. The depth-integrated carbon stock of the longest core (1L) was 95,575 g C/m^2, while Core 2L, which was only 30 cm shorter, contained 75,417 g C/m^2. Core 3L, the shortest core closest to the upland, had 33,356 g C/m^2.

3.2. Creek Bank Cross-Sectional Carbon Profile and Plant Coverage

At the creek bank edge of Traps Bay, the closely spaced short cores (Figure 1d) exhibited a wide range of OC content, from 0.1% to 29.8% (Figure 3a). The upper horizontal layer of marsh sediment (0–20 cm) was lower in carbon content compared to the underlying sediment layers. The creek bank consisted of horizontal layers that increased in carbon content with depth (Figure 3a). The SCD profile reflected the OC profile between 1 and 2 m from the creek bank. However, the 1-m edge of marsh bank closest to the creek bank exhibited lower SCD than the interior 1 m, except for a tongue of higher carbon density at intermediate depths that reached the marsh edge (Figure 3b).

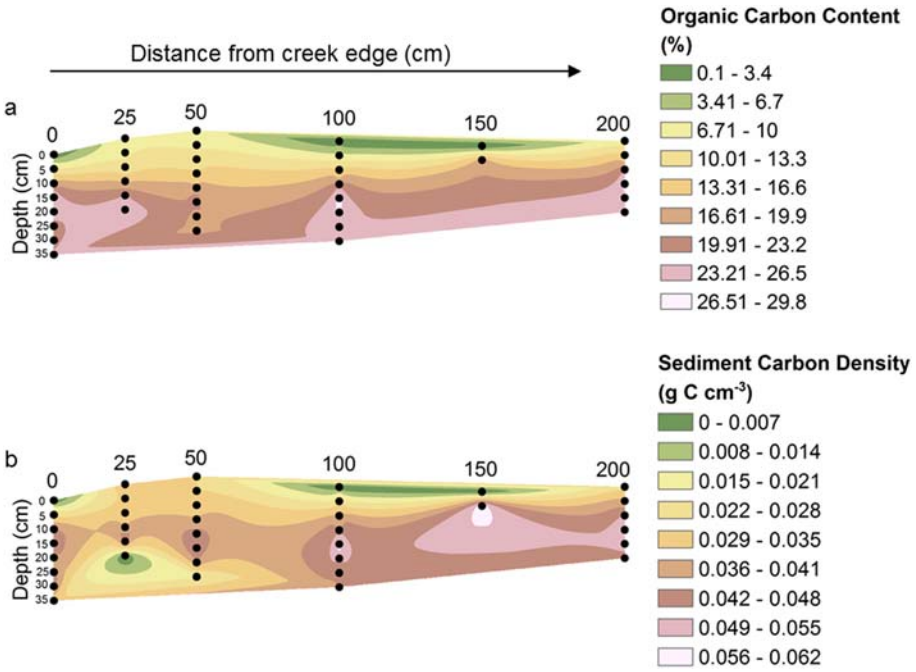

Figure 3. Marsh sediment carbon cross section from short cores taken along the creek bank (denoted at 0 cm) to 200-cm inland. At each 5-cm interval, (a) organic carbon content or (b) sediment carbon density was measured. Values were interpolated between measurement points with inverse distance weighting and displayed in colored contours.

In Traps Bay marsh from 2009 to 2016, the emergent plant community was mixed *S. alterniflora* and *J. roemerianus* (Figure 4). Notably, at the zero transect (i.e., measured across the marsh at the creek bank) beginning in 2013, *S. alterniflora* became more dominant in coverage surveys and remained so through 2016, the last monitoring year. The transects across the marsh at 10 and 20 m from the creek bank were relatively mixed in plant coverage.

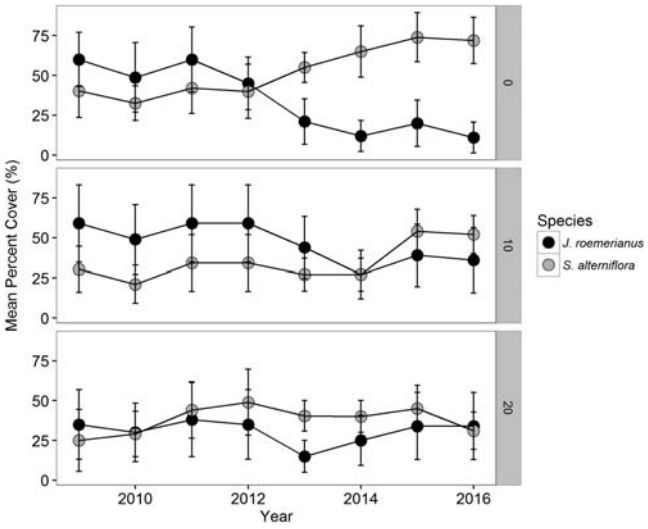

Figure 4. Mean (± s.d.) percent cover for Traps Bay from 2009–2016 for *Juncus roemerianus* and *Spartina alterniflora*. Percent cover was averaged from replicate ($n = 5$) monitoring plots surveyed in mid-July to early August each year. Each replicate plot was situated along parallel transects 0, 10, or 20 m from the creek bank, as designated by the right *y* axis. Surveys used percent cover indicated as Carolina Vegetation Survey category and was converted to the numerical maximum for each category (Peet et al., 2018).

3.3. Marsh Age and CAR

Of the three samples analyzed for ^{14}C age, two were measured at ages approaching modern dates, which indicates that young OM was introduced to the bottom of Cores 2L and 3L. Younger (shallower) material can be accidentally introduced to the bottom of a core by burrowing it during the coring process or retrieving it during the core extraction process. Those samples were omitted from further analysis. Using a linear age-depth model to infer the marsh contact age from the sample age for Core 1L (Johnson et al., 2007), the marsh contact age was estimated at 2460 ± 20 cal BP_{2016} (Table 1). The ^{210}Pb decay curve for Core 2L-Pb resolved the past 109 ± 1 years to 32 cm below the surface (Table 2).

These age-depths cannot be translated into a precise sea level reconstruction since foraminiferal assemblages or another biostratigraphic proxy needed to reconstruct the paleomarsh elevation within the tidal range were not identified. Instead, we inferred past RSLR for this area from a reconstruction completed in a nearby study site (Kemp et al., 2017). The age-depth horizons independently determined by Kemp et al. (2017) using ^{14}C and ^{210}Pb agreed remarkably well with ours (Table 3). Therefore, we justified using the same RSLR estimates from the Kemp et al. study site (Cedar Island) at Traps Bay and using the depth-ages determined by Kemp et al. (2017) to date the bases of Cores 2L and 3L.

Table 2
Comparison of Estimated Ages of Marsh Horizons Between This Study and Kemp et al. (2017)

Core	Geochronology Method from this study	Sample depth from this study (NAVD88, m)	Estimated age range from this study (cal BP_{2016})	Sediment depth from Kemp et al. (2017; NAVD88, m)	Estimated age range from Kemp et al. (2017); cal BP_{2016})
1L	^{14}C	−2.132	2396–2423	−2.116	2423–2683
2L	^{210}Pb	−0.248	107–109	−0.254	90–113

When the Traps Bay salt marsh first formed above Pleistocene sediments thousands of years ago, plants occupied the original surface but marsh plants grew roots into underlying sediments creating a carbon signature deeper than the original marsh surface. This mechanism must be taken into account when reconstructing the ontogeny of the Traps Bay marsh. We estimate that the original marsh surface was 20 cm above the measured marsh basal contact (i.e., we cored past the relict marsh surface to the deepest point of the original marsh rhizosphere). Therefore, the original marsh surfaces in each core can be estimated as 204, 174, and 70 cm below the current marsh surface in Cores 1L, 2L, and 3L, respectively (Figure 5).

The relatively flat surface of the marsh (maximum difference of 2 cm between Cores 1L and 3L) suggests that since initial colonization, the marsh was deposited in horizontal layers that lapped against the upland topography and filled the Traps Bay creek basin. This vertical accretion is visible in the interpolated cross sections as horizontal layers of sediment defined by similar OC and SCD contents (Figures 3a and 3b). Assuming this ontogeny of the marsh, the age of sediment OC stock is uniform across a horizontal planar bed. Therefore, radiocarbon dates represent horizontal planar time horizons that extend across the marsh. Based on the horizontally equal time horizons, we can infer core accretion and CAR for the cores as punctuated rates in sections divided by the time horizons (Figure 5).

Dividing the entire carbon stock of Core 1L (95,575 g C/m^2) by the age of the marsh contact (2,460 ± 20 years cal BP) produces an average annual CAR of 39 ± 0.3 g $C{\cdot}m^{-2}{\cdot}year^{-1}$ (Figure 5). CAR was similarly calculated to be 38 ± 2 and 49 ± 5 g $C{\cdot}m^{-2}{\cdot}year^{-1}$ from the time of marsh origination for Cores 2L and 3L, respectively (Table 1). The OM at 194 cm below the surface of Core 1L was assumed to have the same age as the marsh contact at 194-cm depth in Core 2L (i.e., 1,970 years cal BP_{2016}); therefore, the carbon stock of the top 194 cm in Core 1L divided by the age of the base of the younger Core 2L marsh contact produced a second CAR for that age interval of 41 ± 2 g $C{\cdot}m^{-2}{\cdot}year^{-1}$. In the same way, CAR for the past 680 ± 72 years (i.e., the age of the marsh contact in Core 3L) in Core 1L and 2L was 64 ± 7 and 48 ± 6 g $C{\cdot}m^{-2}{\cdot}year^{-1}$, respectively, and was 49±5 g C m^{-2} y^{-1} for Core 3L (Figure 5).

Table 3
Sediment Properties and Carbon Accumulation Rates for Core 2L-Pb, Using Ages Determined by ^{210}Pb Geochronology

Depth (cm from surface)	Age (cal BP_{2016})	Cumulative OC Stock (g C/m^2)	CAR (g $C{\cdot}m^{-2}{\cdot}year^{-1}$)
2	4.1 ± 0.1	684	167
4	10.6 ± 0.1	1,289	122
6	15.7 ± 0.1	2,087	133
8	21.2 ± 0.2	2,869	135
10	27.1 ± 0.2	3,645	135
12	31.7 ± 0.2	4,379	138
14	35.4 ± 0.2	5,236	148
16	40.4 ± 0.3	6,014	149
18	45.2 ± 0.3	6,710	149
20	49.7 ± 0.3	7,322	147
22	54.1 ± 0.3	7,975	147
24	59.8 ± 0.4	8,576	143
26	68.2 ± 0.4	9,189	135
28	76.4 ± 0.4	9,693	127
30	88.8 ± 0.5	10,256	116
32	108.6 ± 0.7	10,731	99

Note. OC = organic carbon; CAR = carbon accumulation rate.

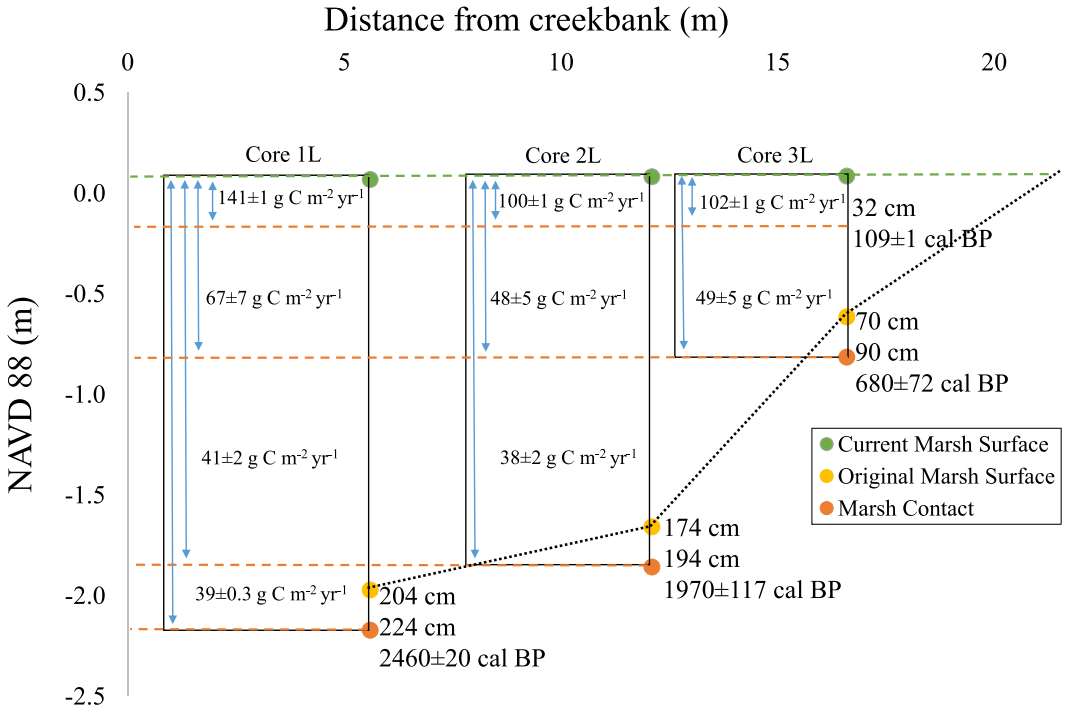

Figure 5. Cross section of three cores collected at Traps Bay plotted by distance from creek bank (*x* axis) and depth (*y* axis). Plotted underneath each core label is the current marsh surface (green circle), estimated original marsh surface (yellow circle), and marsh contact (orange circle) with estimated age. The current marsh surface is represented with a green dashed line. At each marsh contact, a horizontal lamina (orange line) is drawn to intersect the other cores at the same depth representing the same age horizon. Between each age-depth horizon and the current marsh surface, the carbon inventory is given. The black dotted line connects relict marsh surfaces to form the basal Pleistocene paleoshoreline sand unit underlying the current salt marsh.

The estimates of OC stock integrated from surface to every 2-cm depth were matched with the age horizons determined by ^{210}Pb geochronology from depths of 2 to 32 cm (e.g., surface to 2-cm depth, surface to 4-cm depth, ... , surface to 32-cm depth). By this process, CAR was estimated sixteen times in the top 32 cm of the core between 4 cal BP_{2016} and 109 cal BP_{2016} (Table 2). Using only the past 4 years of OM accumulation in the top 2 cm of the core, a CAR of 167 g C·m^{-2}·year^{-1} was determined. However, as the depth of marsh sediment used to calculate CAR increases, CAR decreases. Integrating the top 32 cm of marsh sediment, which accumulated over 109 years, CAR was 99 g C·m^{-2}·year^{-1} (Table 2).

4. Discussion

4.1. Ontogeny of a Salt Marsh

Examination of the preserved OM layers in salt marsh sediments can elucidate both the provenance of that material and the timeline over which that material accumulated, thus, revealing the "ontogeny" of a salt marsh (Redfield, 1965). In Traps Bay, the δ^{13}C values of the OM preserved in the marsh sediment were relatively consistent downcore (Figure 2). All values were more ^{13}C depleted than −20‰, which indicated that the preserved OM was predominantly formed from C_3 vegetation (Cloern et al., 2002; Kemp et al., 2010; Lamb et al., 2006). Interestingly, the dominant emergent vegetation presently at Traps Bay is a mixture of *S. alterniflora*, a C_4 plant, and *J. roemerianus*, a C_3 plant (Figure 4). From plant community monitoring conducted from 2008–2016 CE, *S. alterniflora* replaced *J. roemerianus* as the dominant vegetation type after 2012 at the creek bank (i.e., the 0 transect in Figure 4), possibly from longer inundation times or increased salinity in the creek. Cores 1L, 2L, and 3L were located within the 20-m section of marsh nearest the creek bank where *S. alterniflora* has been present for at least the past 8 years (i.e., since monitoring began). Even in the surface sediment where *S. alterniflora* roots were adding carbon to the sediment, the δ^{13}C values do not reflect the input of C_4 plant material (Figure 2). If *S. alterniflora* persists, then δ^{13}C values would likely become more

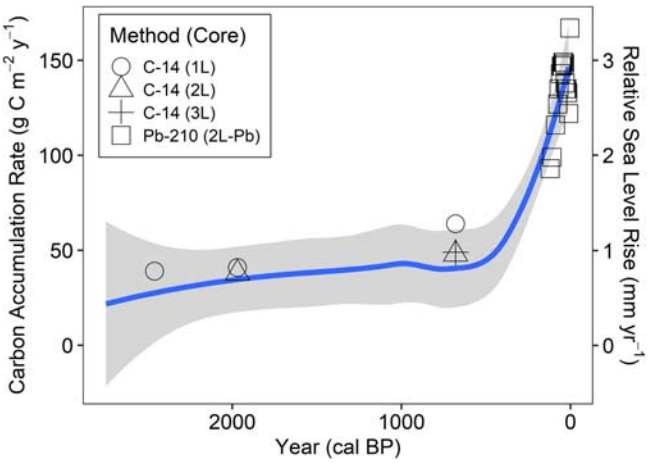

Figure 6. Relationship between carbon accumulation rate estimated by ^{14}C dating in Core 1L (circle), 2L (triangle), 3L (cross), and ^{210}Pb geochronology (squares) with relative sea level rise. Shaded region represents the 95% confidence interval around median relative sea level rise (blue line) fitted with a LOESS function. The year CE 2016 is denoted at $x = 0$.

^{13}C enriched at the marsh surface through time as the concentration of C_4 plant material increases. Possible ^{13}C enrichment in surface sediments was possible from benthic microalgae or cyanobacteria, but if they were present their signature was diluted against the larger OM pool (Cloern et al., 2002; Currin et al., 2011). In Core 2L at 10 cm, the $\delta^{13}C$ value was −20.5‰, which indicates the mixing of C_3 and C_4 plant material, and potential microalgal carbon, which in lower salinity estuarine marshes can have stable C isotope values ranging from −16‰ to −22‰, if that material was preserved upon deposition and subsequent burial (Currin et al., 2003). Detrital *S. alterniflora* is several parts per thousand depleted in ^{13}C compared to live material (Benner et al., 1991; Currin et al., 1995) and only a fraction of the annual belowground biomass produced by wetland plants resists long-term degradation (Davis et al., 2015; Morris & Bowden, 1986). The observed depth profiles of the ^{13}C signature of organic C in the cores are consistent with a small amount of C_4 vegetation diluted against the previously dominant C_3 vegetation.

Based on the sediment OM stable carbon isotope signature, several hypotheses can be devised regarding the historical plant communities that created the carbon stock we measured. Since the stable isotope values reflect almost exclusively C_3 vegetation with some possible mixing of C_4 vegetation, Traps Bay could have been a *Juncus* marsh from its inception until recent *S. alterniflora* colonization. However, using only bulk stable carbon isotopes, it is not possible to decipher *J. roemerianus* from upland maritime forest or other coastal C_3 vegetation (e.g., cypress or cedar forests). Some of the carbon stock in the bottom of the marsh unit could be remnant terrestrial C from when the marsh transgressed upland if the terrestrial C did not completely decompose and/or erode during the period between forest dieback and burial of surface OM by the newly formed marsh. In Core 2L, woody material was recovered between 154 and 160 cm. This material was presumably allochthonous material captured in the marsh, buried, and then preserved in the anoxic sediments before it could decompose. The woody material was of similar $\delta^{13}C$ value (−25.4‰) compared with the OM in the rest of the core but exhibited slightly lower SCD (0.028 g C·cm^{-3}).

4.2. Relating CAR to RSLR

The salt marsh at the study site has persisted there for the past 2,400 years. It has resisted drowning to RSLR for over two millennia via natural ecogeomorphic feedbacks that allow coastal habitats to vertically accrete and keep pace with sea level (Kirwan & Megonigal, 2013). Vertical accretion is a major driver of CAR (Morris et al., 2012; Rogers et al., 2019), as the amount of buried C increases with increased depth (volume) of marsh sediment. Therefore, a positive relationship exists between CAR and RSLR, even as C density remains similar through time (Figures 2 and 6). The OC in Core 1L accumulated over 2,460 ± 20 years, during which RSLR rates were <1 mm/year for >2,000 years before the most recent acceleration of RSLR (Figure 6). While the 2.2-m-deep section of marsh contained a large reservoir of preserved OC, it was accumulated on average at a relatively low rate of 39 ± 0.3 g C·m^{-2}·year^{-1}. Similarly, the OC in Core 2L formed during relatively low rates of RSLR and exhibited relatively low CARs (Figure 6). Compared to the longer Cores 1L and 2L, Core 3L experienced on average a higher rate of RSLR and exhibited a slightly higher CAR (49 ± 5 g C·m^{-2}·year^{-1}); moreover, the sections of Core 1L and 2L from 0–90 cm (i.e., representing the same sediment accumulation horizon as Core 3L) exhibited similar CARs as Core 3L (Table 1 and Figure 5).

Based on the ^{210}Pb geochronology, the uppermost 32 cm of marsh formed over the last 109 ± 1 years and accumulated OC when rates of RLSR were highest since the provenance of the marsh. The CARs over this time period were 141 ± 1.3, 100 ± 0.9, and 102 ± 0.9 g C·m^{-2}·year^{-1} for Cores 1L, 2L, and 3L, respectively (Table 1). Following the trend of accelerating RSLR, each incrementally shallower, thus younger, section of the core exhibited a higher CAR (Figure 6 and Table 2). There are two parts of this mechanism that cannot necessarily be disentangled since we are confounded by simultaneously occurring processes. Rates of CAR

that increase with accelerated RSLR can be attributed to enhanced vertical accretion, an established ecogeomorphic response to RSLR (Kirwan & Mudd, 2012). However, living and/or undecomposed belowground biomass of the salt marsh plants are included in the carbon stock of the near-surface sediment (~20 cm), which corresponds to the sections of highest CAR. While this biomass is part of the belowground carbon stock at the time of sampling, it would inflate long-term CAR if that material would eventually decompose. It is, therefore, inherently impossible to forecast or extrapolate CAR as the future rate of carbon sequestration when using these methods to measure CAR.

While the RSLR data from Kemp et al. (2017) extend to the year 2005 CE, RSLR monitored near the Traps Bay study site show consistently accelerating rates of RSLR. From 2008–2016 CE, areas within 5 km of Traps Bay exhibited RSLR rates as high as 10 and 14 mm/year, which greatly exceed the long-term local average of 3.0 mm/year and is consistent with a *Juncus* to *Spartina* transition (Currin et al., 2018). Furthermore, the region south of Cape Hatteras, NC, which encompasses the current study area, has exhibited sea level rise acceleration to more than 20 mm/year between 2011 and 2015 CE (Valle-Levinson et al., 2017). Similar short-lived, rapid sea level rise accelerations associated with combined cumulative effects of El Niño–Southern Oscillation and North Atlantic Oscillation have occurred at least six times on the U.S. East Coast since 1920 CE (Valle-Levinson et al., 2017). Therefore, the extremely high rates of CAR calculated for the surface sections of the marsh coincide with recent spikes in RSLR. If shallow cores (<20 cm) measuring the recently deposited surface OC from past decades were used to calculate CAR and subsequently extrapolated to the previous century or millennium, the CO_2 storage of the salt marsh would be egregiously inflated. This recent spike of RSLR may also contribute to the change of emergent vegetation species from *J. roemerianus* to the more flood and salt tolerant *S. alterniflora* (Figure 4).

Our millennial CAR estimates align with other studies conducted elsewhere in the United States. Johnson et al. (2007) collected and aged a New England salt marsh core to 3700 cal BP and reported a CAR of 40 g $C{\cdot}m^{-2}{\cdot}year^{-1}$. Brevik and Homburg (2004) collected a core in Southern California that formed over 5,000 years and measured a CAR of 30 g $C{\cdot}m^{-2}{\cdot}year^{-1}$. Likewise, Drexler (2011) measured CAR in cores >6,000 years old and found CARs from 38 to 79 g $C{\cdot}m^{-2}{\cdot}year^{-1}$. In this study, CAR was 39 g $C{\cdot}m^{-2}{\cdot}year^{-1}$ when integrated over ~2,400 years and 2.2-m depth of marsh in Core 1L (Table 1). However, CAR in the surficial 30-cm sections of marsh that accumulated during higher rates of RSLR was up to 3 times higher. For example, the mean rate for the 109 year old, 0- to 32-cm section from Cores 1L, 2L, and 3L was 114 g $C{\cdot}m^{-2}{\cdot}year^{-1}$ compared to 39 g $C{\cdot}m^{-2}{\cdot}y^{-1}$ for the 2,400 year old section of marsh from Core 1L (Table 1). These results demonstrate the carbon storage in salt marshes can be enhanced, at least temporarily, by RSLR-driven OM burial. However, the fate of this material over millennia is unknown. This finding is consistent with the findings of Choi and Wang (2004) who showed centennial CAR measurements (130 ± 9 g $C{\cdot}m^{-2}{\cdot}year^{-1}$) from a Florida *Juncus* marsh were approximately tenfold higher than their CAR measurements integrated over the past 1,820 years (13 ± 2 g $C{\cdot}m^{-2}{\cdot}year^{-1}$).

Methodology biases exist for wetland vertical accretion rates where measurements made over years to decades are usually different for those from the same location made over centuries or millennia (Breithaupt et al., 2018) and evidence exists that the shorter-term marker ^{137}Cs by itself is inadequate to estimate CAR (Drexler et al., 2018). This methodological bias is also inherent in disentangling the changing CARs over time with variations in rates of RSLR. Breithaupt et al. (2018) recommend using multiple timescales with multiple geochronology tools with overlap, if possible, to avoid this. We utilized different methodologies that captured sediment accumulated over different time periods under different RSLR rates. We used both ^{14}C and ^{210}Pb to reconstruct marsh formation; therefore, we can assess variation in CAR at our study site over decades and millennia.

As a conclusion, RSLR is a major driver of CAR in this salt marsh. It is pertinent to measure CAR over timescales that incorporate both environmental (e.g., contemporary RSLR and vegetation change) and biogeochemical processes (e.g., long-term diagenesis) that exhibit control over the rates or OM storage. CAR measured over millennia will likely underestimate contemporary rates if RSLR at the sampling area has increased recently. Conversely, CAR measured over only recent decades that incorporates live belowground biomass into the carbon stock will likely provide overestimated rates for long-term storage budgets since some of that stock will eventually decompose. The challenge then is to balance potentially enhanced rates of accumulation as RSLR accelerates with anticipated degradation processes that will occur over hundreds

of years. We recommend using a geochronology that spans at least 100 years into the past, which is approximately five tidal epochs, to measure CAR so that it will be less influenced by short-term processes like decomposition of labile material. However, based on methodological constraints, CAR, which can only be measured into the past, will always have shortcomings in being used to forecast future rates. These authors caution against meshing short-term (<100 years) CARs with calculations of long-term storage potential (i.e., C emission offsets).

Acknowledgments
This research was conducted under the Defense Coastal/Estuarine Research Program (DCERP), funded by the Strategic Environmental Research and Development Program (SERDP). The scientific results and conclusions, as well as any views or opinions expressed herein, are those of the authors and do not necessarily reflect the views of NOAA or the Department of Commerce and should not be construed as an official U.S. Department of Defense position or decision unless so designated by other official documentation. Raw data used in this study are accessible via the DCERP Data and Information Management System (https://dcerp.rti.org/#/data-portal). J. Ridge and D. Kidwell conducted an internal peer review of this work. Stable isotope analysis was graciously conducted at University of Connecticut by C. Tobias. Several individuals were extremely important in encouraging the development of this manuscript including E. Herbert, M. Kirwan, and I. Anderson. L. Snedaker assisted with laboratory and field work. We are grateful for the constructive feedback from two anonymous reviewers that greatly improved the scope and focus of this work. This research was performed while the corresponding author held an NRC Research Associateship award at the NOAA Center for Coastal Fisheries and Habitat Research Lab.

References

Benner, R., Fogel, M., & Sprague, E. (1991). Diagenesis of belowground biomass of *Spartina alterniflora* in salt-marsh sediments. *Limnology and Oceanography*, *36*(7), 1358–1374. https://doi.org/10.4319/lo.1991.36.7.1358

Blanchard, R. (1966). Rapid determination of lead-210 and polonium-210 in environmental samples by deposition on nickel. *Analytical Chemistry*, *38*(2), 189–192. https://doi.org/10.1021/ac60234a010

Breithaupt, J. L., Smoak, J. M., Byrne, R. H., Waters, M. N., Moyer, R. P., & Sanders, C. J. (2018). Avoiding timescale bias in assessments of coastal wetland vertical change. *Limnology and Oceanography*, *63*(S1), S477–S495. https://doi.org/10.1002/lno.10783

Brevik, E. C., & Homburg, J. A. (2004). A 5000 year record of carbon sequestration from a coastal lagoon and wetland complex, Southern California, USA. *CATENA*, *57*(3), 221–232. https://doi.org/10.1016/j.catena.2003.12.001

Chmura, G. L., Anisfeld, S. C., Cahoon, D. R., & Lynch, J. C. (2003). Global carbon sequestration in tidal, saline wetland soils. *Global Biogeochemical Cycles*, *17*(4), 1111. https://doi.org/10.1029/2002GB001917

Choi, Y., & Wang, Y. (2004). Dynamics of carbon sequestration in a coastal wetland using radiocarbon measurements: Dynamics of carbon sequestration. *Global Biogeochemical Cycles*, *18*, GB4016. https://doi.org/10.1029/2004GB002261

Cloern, J. E., Canuel, E. A., & Harris, D. (2002). Stable carbon and nitrogen isotope composition of aquatic and terrestrial plants of the San Francisco Bay estuarine system. *Limnology and Oceanography*, *47*(3), 713–729. https://doi.org/10.4319/lo.2002.47.3.0713

Craft, C. B., Seneca, E. D., & Broome, S. W. (1991). Loss on ignition and Kjeldahl digestion for estimating organic carbon and total nitrogen in estuarine marsh soils: Calibration with Dry Combustion. *Estuaries*, *14*(2), 175. https://doi.org/10.2307/1351691

Crooks, S., Herr, D., Tamelander, J., Laffoley, D., & Vandever, J. (2011). Mitigating climate change through restoration and management of coastal wetlands and near-shore marine ecosystems—Challenges and opportunities (Environment Department Papers No. 121) (p. 69). Washington, D.C.: The World Bank.

Currin, C., Levin, L. A., Talley, T. S., Michener, R., & Talley, D. (2011). The role of cyanobacteria in Southern California salt marsh food webs: Cyanobacteria in marsh food webs. *Marine Ecology*, *32*(3), 346–363. https://doi.org/10.1111/j.1439-0485.2011.00476.x

Currin, C., Newell, S., & Paerl, H. (1995). The role of standing dead *Spartina alterniflora* and benthic microalgae in salt marsh food webs: Considerations based on multiple stable isotope analysis. *Marine Ecology Progress Series*, *121*, 99–116. https://doi.org/10.3354/meps121099

Currin, C. A., Hilting, A., Greene, M., & Ensign, S. (2018). Coastal wetland monitoring program. In P. Cunningham (Ed.), *Defense coastal/estuarine research program 2 final report (Chapter 11)* (pp. 1–59). Raleigh, N.C: RTI International.

Currin, C. A., Wainright, S. C., Able, K. W., Weinstein, M. P., & Fuller, C. M. (2003). Determination of food web support and trophic position of the mummichog, Fundulus heteroclitus, in New Jersey smooth cordgrass (Spartina alterniflora), common reed (Phragmites australis), and restored salt marshes. *Estuaries*, *26*(2), 495–510. https://doi.org/10.1007/BF02823726

Davis, J. L., Currin, C. A., O'Brien, C., Raffenburg, C., & Davis, A. (2015). Living shorelines: Coastal resilience with a blue carbon benefit. *PLOS ONE*, *10*(11). https://doi.org/10.1371/journal.pone.0142595

Donato, D. C., Kauffman, J. B., Murdiyarso, D., Kurnianto, S., Stidham, M., & Kanninen, M. (2011). Mangroves among the most carbon-rich forests in the tropics. *Nature Geoscience*, *4*(5), 293–297. https://doi.org/10.1038/ngeo1123

Drexler, J. Z. (2011). Peat formation processes through the millennia in tidal marshes of the Sacramento–San Joaquin Delta, California, USA. *Estuaries and Coasts*, *34*(5), 900–911. https://doi.org/10.1007/s12237-011-9393-7

Drexler, J. Z., Fuller, C. C., & Archfield, S. (2018). The approaching obsolescence of Cs-137 dating of wetland soils in North America. *Quaternary Science Reviews*, *199*, 83–96. https://doi.org/10.1016/j.quascirev.2018.08.028

Duarte, C. M., Middelburg, J. J., & Caraco, N. (2005). Major role of marine vegetation on the oceanic carbon cycle. *Biogeosciences Discussions*, *1*.

El-Daoushy, F., Olsson, K., & Garciatenorio, R. (1991). Accuracies in Po-210 Determination for Pb-210 Dating. *Hydrobiologia*, *214*(1), 43–52. https://doi.org/10.1007/BF00050930

Flynn, W. W. (1968). The determination of low levels of Polonium-210 in environmental materials. *Analytica Chimica Acta*, *43*, 221–227.

Gehrels, W. R. (1999). Middle and Late Holocene sea-level changes in Eastern Maine reconstructed from foraminiferal saltmarsh stratigraphy and AMS 14C dates on basal peat. *Quaternary Research*, *52*(3), 350–359. https://doi.org/10.1006/qres.1999.2076

Holmquist, J. R., Windham-Myers, L., Bliss, N., Crooks, S., Morris, J. T., Megonigal, J. P., et al. (2018). Accuracy and precision of tidal wetland soil carbon mapping in the conterminous United States. *Scientific Reports*, *8*(1), 9478. https://doi.org/10.1038/s41598-018-26948-7

Howard, J., Sutton-Grier, A., Herr, D., Kleypas, J., Landis, E., Mcleod, E., et al. (2017). Clarifying the role of coastal and marine systems in climate mitigation. *Frontiers in Ecology and the Environment*, *15*(1), 42–50. https://doi.org/10.1002/fee.1451

Johnson, B. J., Moore, K. A., Lehmann, C., Bohlen, C., & Brown, T. A. (2007). Middle to late Holocene fluctuations of C3 and C4 vegetation in a Northern New England Salt Marsh, Sprague Marsh, Phippsburg Maine. *Organic Geochemistry*, *38*(3), 394–403. https://doi.org/10.1016/j.orggeochem.2006.06.006

Kemp, A. C., Kegel, J. J., Culver, S. J., Barber, D. C., Mallinson, D. J., Leorri, E., et al. (2017). Extended late Holocene relative sea-level histories for North Carolina, USA. *Quaternary Science Reviews*, *160*, 13–30. https://doi.org/10.1016/j.quascirev.2017.01.012

Kemp, A. C., Vane, C. H., Horton, B. P., & Culver, S. J. (2010). Stable carbon isotopes as potential sea-level indicators in salt marshes, North Carolina, USA. *The Holocene*, *20*(4), 623–636. https://doi.org/10.1177/0959683609354302

Kirwan, M. L., & Guntenspergen, G. R. (2012). Feedbacks between inundation, root production, and shoot growth in a rapidly submerging brackish marsh: MARSH ROOT GROWTH UNDER SEA LEVEL RISE. *Journal of Ecology*, *100*(3), 764–770. https://doi.org/10.1111/j.1365-2745.2012.01957.x

Kirwan, M. L., & Megonigal, J. P. (2013). Tidal wetland stability in the face of human impacts and sea-level rise. *Nature*, *504*(7478), 53–60. https://doi.org/10.1038/nature12856

Kirwan, M. L., & Mudd, S. M. (2012). Response of salt marsh carbon accumulation to climate change. *Nature*, *489*(7417), 550–553. https://doi.org/10.1038/nature11440

Lamb, A. L., Wilson, G. P., & Leng, M. J. (2006). A review of coastal palaeoclimate and relative sea-level reconstructions using δ13C and C/N ratios in organic material. *Earth-Science Reviews*, *75*(1–4), 29–57. https://doi.org/10.1016/j.earscirev.2005.10.003

Martin, P., & Hancock, G. J. (2004). Peak resolution and tailing in alpha-particle spectrometry for environmental samples. *Applied Radiation and Isotopes*, *61*(2–3), 161–165. https://doi.org/10.1016/j.apradiso.2004.03.038

Matthews, K. M., Kim, C.-K., & Marin, P. (2007). Determination of ^{210}Po in environmental materials: A review of analytical methodology. *Applied Radiation and Isotopes*, *65*(3), 267–279.

Mcleod, E., Chmura, G. L., Bouillon, S., Salm, R., Björk, M., Duarte, C. M., et al. (2011). A blueprint for blue carbon: toward an improved understanding of the role of vegetated coastal habitats in sequestering CO $_2$. *Frontiers in Ecology and the Environment*, *9*(10), 552–560. https://doi.org/10.1890/110004

Morris, J. T., & Bowden, W. B. (1986). A mechanistic, numerical model of sedimentation, mineralization, and decomposition for marsh sediments. *Soil Science Society of America Journal*, *50*(1), 96–105. https://doi.org/10.2136/sssaj1986.03615995005000010019x

Morris, J. T., Edwards, J., Crooks, S., & Reyes, E. (2012). Assessment of carbon sequestration potential in coastal wetlands. In R. Lal, K. Lorenz, R. F. Hüttl, B. U. Schneider, & J. von Braun (Eds.), *Recarbonization of the biosphere* (pp. 517–531). Dordrecht: Springer Netherlands. https://doi.org/10.1007/978-94-007-4159-1_24

Morris, J. T., Sundareshwar, P. V., Nietch, C. T., Kjerfve, B., & Cahoon, D. R. (2002). Responses of coastal wetlands to rising sea level. *Ecology*, *83*(10), 2869–2877. https://doi.org/10.1890/0012-9658(2002)083[2869:ROCWTR]2.0.CO;2

Nellemann, C. (2009). *Blue carbon: The role of healthy oceans in binding carbon: A rapid response assessment (A Rapid Response Assessment)*. Norway: Birkeland Trykkeri AS. Retrieved from. www.grida.no

Neumeier, U., & Ciavola, P. (2004). Flow resistance and associated sedimentary processes in a Spartina maritima salt-marsh. *Journal of Coastal Research*, *20*(2), 435–447.

Nixon, S. W., & Oviatt, C. A. (1973). Ecology of a New England salt marsh. *Ecological Monographs*, *43*(4), 463–498. https://doi.org/10.2307/1942303

Oertel, G. F., Wong, G. T. F., & Conway, J. D. (1989). Sediment accumulation at a fringe marsh during transgression, Oyster, Virginia. *Estuaries*, *12*(1), 18. https://doi.org/10.2307/1351446

Ouyang, X., & Lee, S. Y. (2014). Updated estimates of carbon accumulation rates in coastal marsh sediments. *Biogeosciences*, *11*(18), 5057–5071. https://doi.org/10.5194/bg-11-5057-2014

Peet, R. K., Palmquist, K. A., Wentworth, T. R., Schafale, M. P., Weakley, A. S., & Lee, M. T. (2018). Carolina Vegetation Survey: An initiative to improve regional implementation of the US National Vegetation Classification. *Phytocoenologia*, *48*(2), 171–179. https://doi.org/10.1127/phyto/2017/0168

Pethick, J. S. (1981). Long-term accretion rates on tidal salt marshes. *Journal of Sedimentary Petrology*, *51*(2). https://doi.org/10.1306/212F7CDE-2B24-11D7-8648000102C1865D

Redfield, A. C. (1965). Ontogeny of a salt marsh estuary. *Science*, *147*(3653), 50–55. https://doi.org/10.1126/science.147.3653.50

Reimer, P. J., Bard, E., Bayliss, A., Beck, J. W., Blackwell, P. G., Ramsey, C. B., et al. (2013). IntCal13 and Marine13 radiocarbon age calibration curves 0–50,000 Years cal BP. *Radiocarbon*, *55*(4), 1869–1887. https://doi.org/10.2458/azu_js_rc.55.16947

Rogers, K., Kelleway, J. J., Saintilan, N., Megonigal, J. P., Adams, J. B., Holmquist, J. R., et al. (2019). Wetland carbon storage controlled by millennial-scale variation in relative sea-level rise. *Nature*, *567*(7746), 91–95. https://doi.org/10.1038/s41586-019-0951-7

Sadler, P. M. (1981). Sediment accumulation rates and the completeness of stratigraphic sections. *The Journal of Geology*, *89*(5), 569–584. https://doi.org/10.1086/628623

Sanchez-Cabeza, J. A., Masqué, P., & Ani-Ragolta, I. (1998). ^{210}Pb and ^{210}Po analysis in sediments and soils by microwave acid digestion. *Journal of Radioanalytical and Nuclear Chemistry*, *227*(1-2), 19–22. https://doi.org/10.1007/BF02386425

Stuiver, M., & Polach, H. A. (1977). Discussion reporting of ^{14}C data. *Radiocarbon*, *19*(3), 355–363. https://doi.org/10.1017/S0033822200003672

Trumper, K., Bertzky, M., Dickson, B., van der Heijden, G., Jenkins, M., & Manning, P. (2009). The natural fix? The role of ecosystems in climate mitigation: A UNEP rapid response assessment (A UNEP Rapid Response Assessment). Cambridge, U.K: United Nations Environment Programme.

Valle-Levinson, A., Dutton, A., & Martin, J. B. (2017). Spatial and temporal variability of sea level rise hot spots over the eastern United States. *Geophysical Research Letters*, *44*, 7876–7882. https://doi.org/10.1002/2017GL073926

van de Plassche, O., van der Borg, K., & de Jong, A. F. M. (1998). Sea level–climate correlation during the past 1400 yr. *Geology*, *26*(4), 319. https://doi.org/10.1130/0091-7613(1998)026<0319:SLCCDT>2.3.CO;2

Winker, C. D., & Howard, J. D. (1977). Correlation of tectonically deformed shorelines on the southern Atlantic coastal plain. *Geology*, *5*(2), 123–127. https://doi.org/10.1130/0091-7613(1977)5<123:COTDSO>2.0.CO;2